Lithos 106 (2008) 83–92

Contents lists available at ScienceDirect

Lithos

journal homepage: www.elsevier.com/locate/lithos

Was there Jurassic paleo-Pacific subduction in South China?: Constraints from $^{40}Ar/^{39}Ar$ dating, elemental and Sr–Nd–Pb isotopic geochemistry of the Mesozoic basalts

Cheng-Hong Chen [a,*], Chi-Yu Lee [a], Ryuichi Shinjo [b]

[a] Department of Geosciences, National Taiwan University, Taipei, Taiwan
[b] Department of Physics and Earth Sciences, University of the Ryukyus, Okinawa, Japan

ARTICLE INFO

Article history:
Received 15 February 2008
Accepted 9 June 2008
Available online 25 June 2008

Keywords:
Mesozoic basalts
Cathaysia
South China
Paleo-Pacific subduction

ABSTRACT

There is an ongoing debate concerning whether the vast Nanling Mountain granitoids of South China are the result of Jurassic paleo-Pacific subduction. We address this question by examining two Mesozoic basalt successions in South China, one parallel and the other oblique to the convergence boundary between the paleo-Pacific plate and South China continent. The geochemical characteristics of these basalts are used to constrain the influence of this presumed subduction system on mantle composition. $^{40}Ar/^{39}Ar$ age, major element and trace element abundances, and Sr, Nd and Pb isotope data indicate that the northeast-southwest trending basalts in the Southeast Coast Magmatic Belt that formed during 101–76 Ma exhibit arc-like signatures and are derived from subduction-modified mantle. However, the east–west trending basalt array extending from the Cathaysia Interior to the Cathaysia Folded Belt, which decreases in age from 175 to 98 Ma in an eastward direction, is characterized by lithosphere-modified OIB-like asthenosphere composition, except for a few younger rocks from Huichang which resemble Southeast Coast Magmatic Belt basalts. These results suggest that the Jurassic mantle beneath the Cathaysia Interior and the Cathaysia Folded Belt was rather homogeneous and undisturbed, and was not affected by the paleo-Pacific subduction system. Alternatively, post-orogenic (Indosinian) extension accompanied by mafic underplating may have been the cause of vast Jurassic granitic magmatism in South China.

1. Introduction

South China is a continental block formed by the amalgamation of Yangtze and Cathaysia Blocks in the Neoproterozoic–Paleozoic. The Cathaysia Block is composed mainly of Mesozoic granitoids-volcanic rocks with a total area of ~220,000 km^2 (Zhou et al., 2006). Traditionally, Mesozoic granitoids in South China (Triassic 16%, Jurassic 47%, and Cretaceous 37%; Fig. 1a) were thought to have resulted from staged orogenic cycles under prolonged, low-angle, and west-dipping subduction of the paleo-Pacific plate, based on the observation that these rocks decrease in age in an eastwardly direction (Zhou and Li, 2000; Li and Li, 2007). However, other observations seem to conflict with this flat subduction model. For instance, Triassic granitoids are widespread in South China (Chen et al., 2006); and the Early Jurassic was basically a non-magmatic stage in the Cathaysia Block (Zhou et al., 2006). The convergence vector determined from paleomagnetic data was in the northwest direction for paleo-Pacific subduction during 175–150 Ma (Ratschbacher et al., 2000); and Jurassic magmatism, exemplified by the vast Nanling Mountain granitoids, was largely concentrated at ca.160 Ma (Xu et al., 2005).

During the Mesozoic, intermittent basic eruptions, generally in association with silicic volcanism, occurred in the Cathaysia Block. Because basaltic rocks are good indicators of mantle composition, the study of these rocks can provide information on mantle composition and directly reveal whether the mantle beneath this Block has incorporated a subducted component. Therefore, we measured $^{40}Ar/^{39}Ar$ age, major and trace elements, and Sr, Nd and Pb isotope ratios from basalts in the region that had previously not been studied in detail. Combined with related data from the literature, the new data is used to document the spatial and temporal distribution of Mesozoic basalts and constrain the characteristics of the mantle beneath South China. This approach enables us to evaluate the influence of Jurassic paleo-Pacific subduction.

2. Geological background and sample localities

The Cathaysia Block can be separated into the Cathaysia Interior, Cathaysia Folded Belt and Southeast Coast Magmatic Belt by two tectonic lines, the Shi-Hang Zone and the Lishui-Haifeng Fault (Fig. 1a). The fact that Triassic granitic rocks (S-type) are mainly distributed in the Cathaysia Interior and Cathaysia Folded Belt, Cretaceous rocks (I-type) in the Southeast Coast Magmatic Belt, and Jurassic rocks

* Corresponding author. Department of Geosciences, National Taiwan University, No.1, Roosevelt Road Section 4, Taipei 106, Taiwan. Tel.: +886 2 3366 5872; fax: +886 2 2363 6095.
E-mail address: chench@ntu.edu.tw (C.-H. Chen).

0024-4937/$ – see front matter © 2008 Elsevier B.V. All rights reserved.
doi:10.1016/j.lithos.2008.06.009

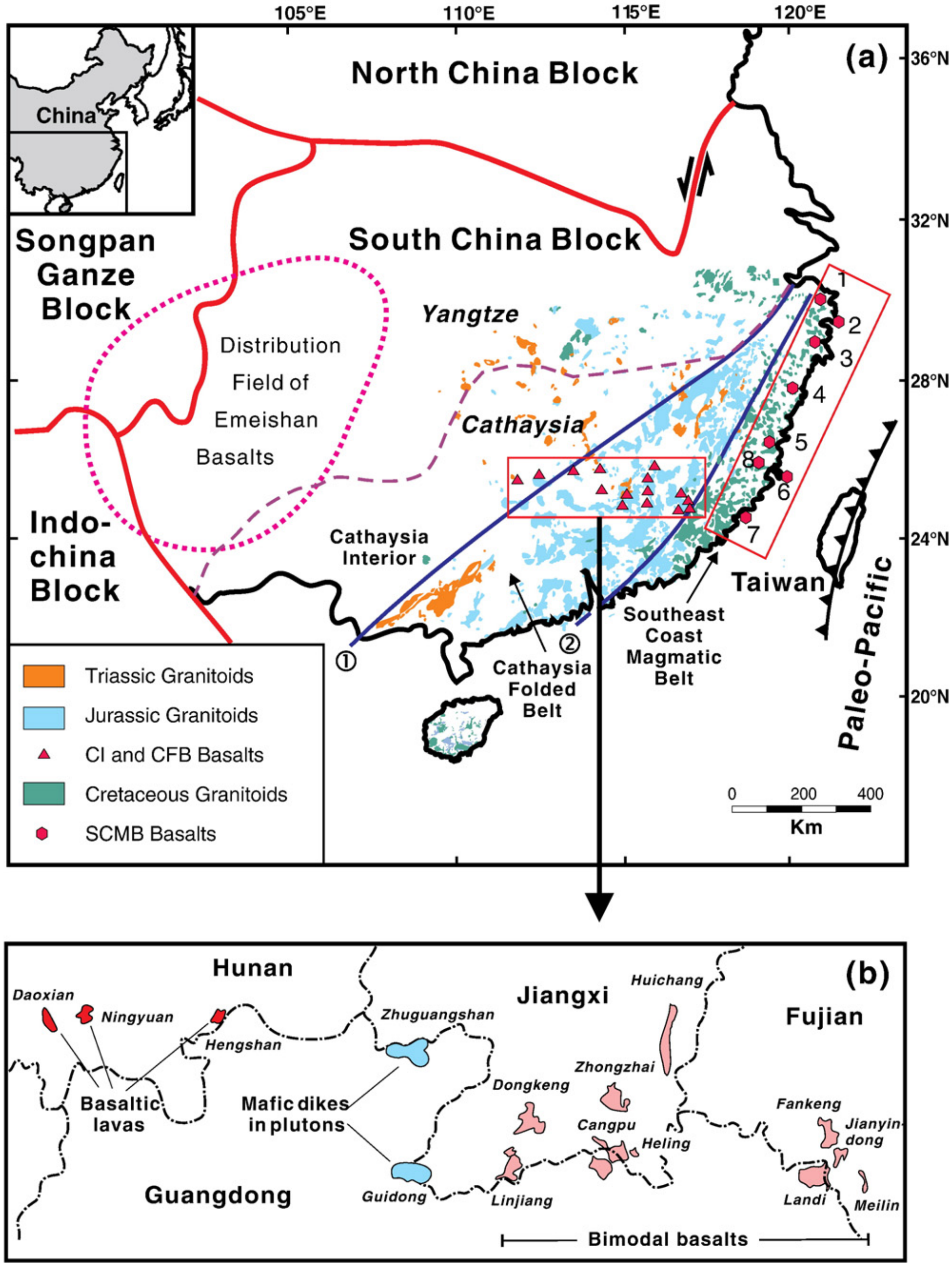

Fig. 1. (a) Map showing Mesozoic granitoids of the South China Block (modified from Zhou et al., 2006; Li and Li, 2007) and distribution of Permo/Triassic Emeishan basalts. The South China Block is comprised of two smaller Blocks: Yangtze and Cathaysia. The Shi-Hang Zone (1) and the Lishui-Haifeng Fault (2) further separate the Cathaysia Block into three tectonic units: Cathaysia Interior (CI), Cathaysia Folded Belt (CFB), and Southeast Coast Magmatic Belt (SCMB). Sample locations of studied basaltic rocks are denoted as triangles in the Cathaysia Interior and Cathaysia Folded Belt and polygons in the Southeast Coast Magmatic Belt. The chain-saw symbol along Taiwan is a presumed Cretaceous subduction zone of the paleo-Pacific plate. (b) The enlarged area of the east-west basalt array. Detailed location map of the northeast–southwest basalt array in the Southeast Coast Magmatic Belt (1: Xuentandi, 2: Pingyen, 3: Tientai, 4: Shanmeng, 5: Kuiqi, 6: Matsu, 7: Chinmen, and 8: Yongtai) can be seen in Chen et al. (2008).

(intermediary type) in the Cathaysia Folded Belt has been the basis for tectonic models of Mesozoic Cathaysia. Lithologically, the vast Late Jurassic granitoids are predominately biotite granites of high-K calc-alkaline affinity. The presence of Early Jurassic aluminous A-type granites, gabbros, syenitic rocks, and intraplate basalts in Hunan and Jiangxi is an indication of the development of continental extension or intraplate rifting in the western Cathaysia Folded Belt (Li et al., 2003, 2004; Wang et al., 2003, 2005). Yet the timing of such an extensional environment in the eastern Cathaysia Folded Belt is not well constrained. In the Southeast Coast Magmatic Belt, magmatism was characterized by shallow intrusions of voluminous I-type granitoids at 110–99 Ma and subsequent near-surface emplacement of A-type granites with eruptions of silicic-dominated bimodal volcanic suites and injections of mafic dikes (Martin et al., 1994; Chen et al., 2008). The time sequence and rock type relationships observed in South China are consistent with subduction-driven thermal activity that developed in the post- to anorogenic extensional stages of an active continental margin (Zhou and Li, 2000; Chen et al., 2004).

Basaltic rocks in the Southeast Coast Magmatic Belt are distributed along the southeast China coastal area as an array extending for ~700 km parallel to the northeast–southwest trending convergence plate boundary of the paleo-Pacific subduction system. Here we focus on another array of basaltic rocks outcropping across the Cathaysia Interior and Cathaysia Folded Belt for ~550 km, oblique to the plate boundary (Fig. 1a). The former consist of basaltic lavas intercalated with rhyolites (Xuentandi, Pingyen, Teintai, Shanmeng and Yongtai) and mafic dikes intruding Cretaceous granitic plutons (Kuiqi, Matsu and Chinmen). The latter include various types of basaltic rock distributed from south Hunan (lavas in Daoxian, Ningyuan and Hengshan), through north Guangdong (mafic dikes in Zhuguangshan and Guidong), south Jiangxi (basalt/rhyolite bimodal suites in Linjiang-Dongkeng, Huichang, Zhongzhai and Heling), to southeast Fujian (similar bimodal suites in Fankeng, Jianyindong, Landi and Meilin) (Fig. 1b). Permo/Triassic Emeishan basalts (Xu et al., 2007) are widespread in the western part of the South China Block over an area of about 250,000 km^2 (Fig. 1a) and their relationship to Mesozoic mantle evolution is also considered here.

3. Analytical methods

Fresh basalt chips were dated using the step-heating $^{40}Ar/^{39}Ar$ age spectrum technique described by Lo and Lee (1994) to establish the time of basaltic volcanism. These dating analyses were performed using a Varian® MAT GD150 mass spectrometer at National Taiwan University (NTU). Results of the $^{40}Ar/^{39}Ar$ incremental heating experiments for the Cathaysia Folded Belt basalts are shown in Appendix 1. Major element composition was determined on fused glass disks by the X-ray fluorescence technique using a Rigaku® RIX 2000 spectrometer and trace element abundances ware measured on a digested solution by inductively coupled plasma-mass spectrometry using a Perkin Elmer® Elan-6000 spectrometer at NTU. Ratios of $^{87}Sr/^{86}Sr$ and $^{143}Nd/^{144}Nd$ isotope were measured using a Finnigan® MAT 262 mass spectrometer at National Cheng Kung University. Details for all these analytical methods have been previously described by Chen et al. (2004, 2008). Lead isotope measurements were made on a Finnigan® MAT 262 mass spectrometer at the University of the Ryukyus. Lead isotopic ratios were corrected for mass fractionation using a ^{204}Pb–^{207}Pb double spike with $^{207}Pb/^{204}Pb = \sim 1$. The procedure is similar to that described in Woodhead et al. (1995). Fractionation-corrected ratios measured for NBS-981 ($n = 3$) were $^{206}Pb/^{204}Pb = 16.9403$ (±0.0004 at the 2σ level), $^{207}Pb/^{204}Pb = 15.4976$ (±0.0005), and $^{208}Pb/^{204}Pb = 36.7195$ (±0.0022). Results of elemental and isotopic analyses of representative samples for Cathaysia Folded Belt and Southeast Coast Magmatic Belt basalts, together with some Emeishan and Cathaysia Interior basalt data from the literature, are presented in Appendix 2.

4. $^{40}Ar/^{39}Ar$ dating results

Relevant rocks with known ages include Emeishan basalts: 259 – 251 Ma (Xu et al., 2007 and references therein); south Hunan basalts: summarized as ~175 Ma (Ningyuan), ~150 Ma (Daoxian) and ~125 Ma (Hengshan) (Wang et al., 2003; Li et al., 2004); and north Guangdong mafic dikes in three stages: ~140, ~105 and ~90 Ma (Li and McCulloch, 1998). In the Southeast Coast Magmatic Belt, basaltic eruptions (101–81 Ma) and mafic dike injections (94–76 Ma) took place nearly simultaneously over the entire belt (Chen et al., 2008). Basically, all these ages were obtained using the $^{40}Ar/^{39}Ar$ age spectrum technique, except for a few analyses of the Emeishan plume eruption (~259 Ma) which were obtained from the most reliable SHRIMP U/Pb zircon age dates (Ali et al., 2005 and references therein).

Our new $^{40}Ar/^{39}Ar$ age data on eight Cathaysia Folded Belt basalts, which are based on well-developed plateau ages, reveal that they erupted in two stages at 137 – 123 Ma (Fig. 2a–d) and 108–98 Ma (Fig. 2e–h), respectively. The timing of these two basaltic cycles fairly closely matches the north Guangdong mafic dike injections at ~140 and 105 Ma, respectively, probably indicating that episodic heat pulses occurred in the Cathaysia Folded Belt. Spatially, stage-1 and -2 basalts are more concentrated in the central and eastern parts of the east–west basalt array (Fig. 1b). Such an eastwardly age-decreasing trend differs greatly from the previous view that all the Cathaysia Interior and Cathaysia Folded Belt basalts erupted simultaneously at ca. 180–170 Ma (e.g., Xie et al., 2006).

5. Geochemical and isotopic results and interpretations

The tectonic settings of the Permo/Triassic Emeishan and Late Cretaceous Southeast Coast Magmatic Belt basalts in South China are well established as mantle plume derived (Xu et al., 2007) and paleo-Pacific plate subduction (Chen et al., 2008) events, respectively. In this study we focus on the major and trace elements, and Sr, Nd and Pb isotopic compositions of the Cathaysia Interior and Cathaysia Folded Belt basalts, particularly those distributed in south Jiangxi to southwest Fujian. The basalts of the Southeast Coast Magmatic Belt are mostly alkaline ($Na_2O + K_2O > 3.8$ wt.%), whereas the Emeishan basalts are largely subalkaline ($Na_2O + K_2O < 4.9$ wt.%) (Fig. 3a): a common feature of flood basalts (Xu et al., 2001). The Southeast Coast Magmatic Belt basalts and the Emeishan basalts are more clearly distinguished on a TiO_2 vs. Al_2O_3 plot (Fig. 3b): Southeast Coast Magmatic Belt basalts have a high Al_2O_3 (>15.2 wt.%) and low TiO_2 (<2.5 wt.%) content as do island arc basalts (IAB), and Emeishan basalts have a low Al_2O_3 but variable TiO_2 content. All these major element characteristics may reflect first-order processes related to their mantle sources with or without involvement of significant fluids expelled from the subducted slab, as subduction modified magmas are often enriched in Al_2O_3 by plagioclase accumulation, and plagioclase nucleation may be delayed, depending on the H_2O content (Crawford et al., 1987). The TiO_2 variability is probably related to the FeO content of the iron oxide phases in the basalts. Early crystallization and separation of magnetite at high oxygen fugacity can cause a calc-alkaline differentiation trend, which is more pronounced at high water content (Berndt et al., 2005). Therefore, the high-Al, low-Ti character of Southeast Coast Magmatic Belt basalts reflects a relatively high-H_2O environment, most probably contributed by the subducted slab.

Basalts of the east–west array overlap Emeishan and Southeast Coast Magmatic Belt basalts in terms of alkalinity, and have intermediate compositions straddling the Al_2O_3 boundary (at 15.2 wt.%) between these two basalt distribution fields. In the Cathaysia Interior section, Ningyuan basalts exclusively fall in the Emeishan field; however, Daoxian basalts show extremely low Al_2O_3 and TiO_2 content. Along with high MgO content (>16 wt.%), Daoxian basalts are similar to the unusual low-Ti, high-Mg basalts in the Deccan Traps that were explained by involving significant crustal input (Mellusoa et al., 2006; see later sections). In the Cathaysia Folded Belt section, some samples occupy the high Al_2O_3 and TiO_2 quadrant where no Emeishan and Southeast Coast Magmatic Belt basalts are situated; others, like the Huichang basalts from south Jiangxi, retain their high aluminous character but have low TiO_2 content down to 0.9 – 1.0 wt.% (6 analyses). These features reflect the complexity of Cathaysia Interior and Cathaysia Folded Belt basalts.

Trace element behaviors of these basalts are best exemplified by the primitive mantle-normalized multi-element distribution pattern (Fig. 4) using Emeishan basalts (Xu et al., 2001; Ali et al., 2005) as the reference (the shaded pattern). Ningyuan basalts have slightly higher concentrations of incompatible trace elements, such as Ba, Th, U, Nb, Ta, Sr and LREE, than the north Guangdong mafic dikes and Cathaysia Folded Belt basalts (excluding those from Huichang), which are in general, similar to Emeishan basalts (Fig. 4a–c). Such geochemical features of Ningyuan basalts resemble those of typical ocean island basalts (OIB) (McDonough and Sun, 1995). On the other hand, Southeast Coast Magmatic Belt basaltic rocks are characterized by slight but diagnostic Nb–Ta–Ti depletions, as in IAB, indicative of subduction-related processes for their magma generation. It is noted that Huichang basalts possess the same Nb–Ta–Ti depletions as Southeast Coast Magmatic Belt basaltic rocks. However, the lack of Th and U depletions in Huichang basalts (Fig. 4d) makes them

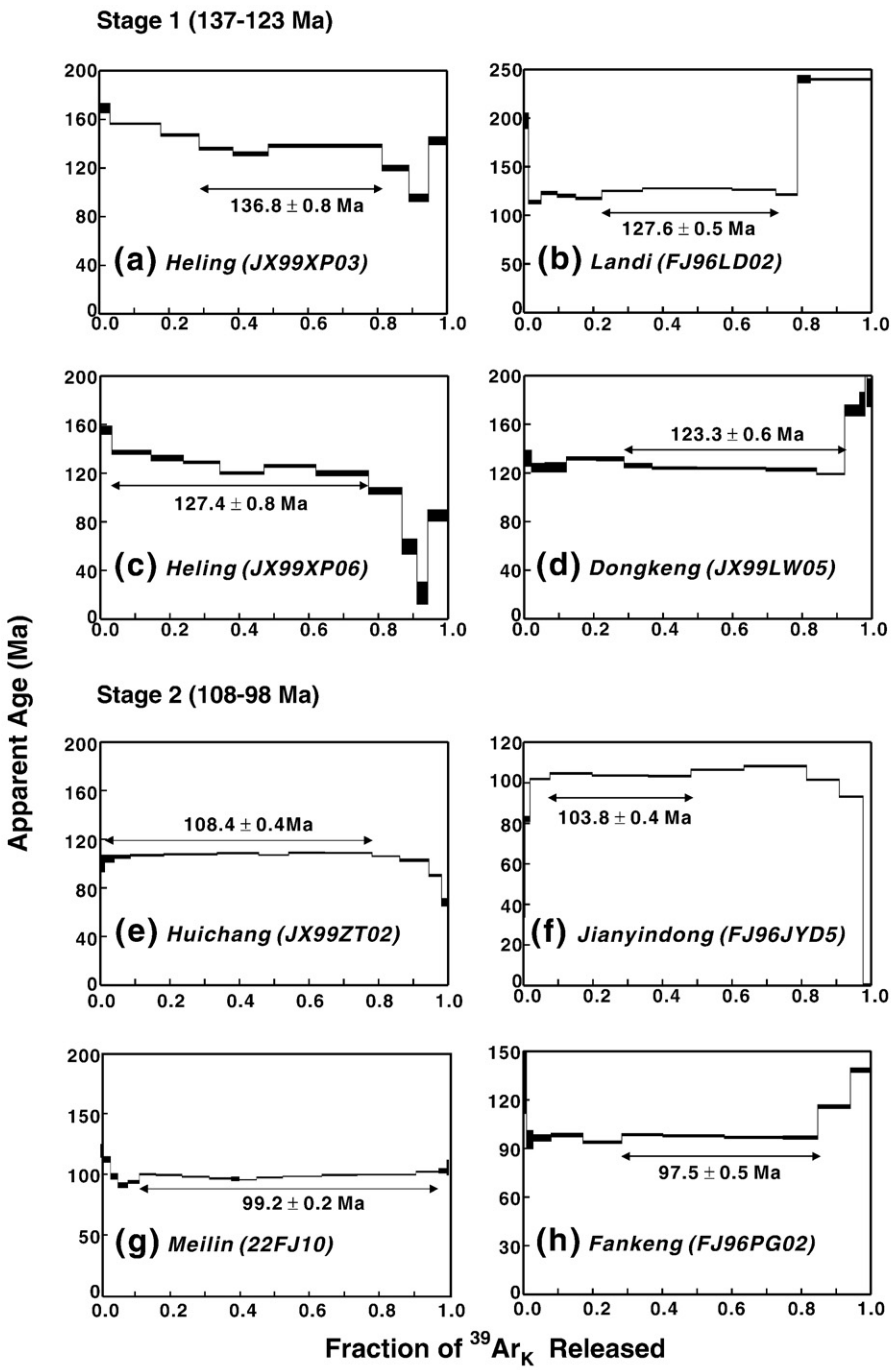

Fig. 2. $^{40}Ar/^{39}Ar$ plateau ages for some Cathaysia Folded Belt basalts in South China, with source data in Appendix 1. Localities and chemical compositions of each rock sample can be found in Fig. 1 and in Appendix 2.

distinguishable from the latter rocks (Fig. 4e–f). These basalts may be more influenced by fluid- than sediment-dominant fluxes from the subducted slab at a greater distance from subduction zone (Turner and Hawkesworth, 1997). On this basis, Mesozoic basaltic rocks in South China with arc signatures first appeared in the central part of the Cathaysia Folded Belt at 108 Ma, or the earliest phase of stage-2 basaltic eruptions. In the following we combine one of the most sensitive trace element discriminators of tectonic environments, the La/Nb ratio, with Nd isotope data to further delineate mantle sources for these basalts.

Based on Os, Pb and Nd isotopic compositions, Emeishan basalts are suggested to have been generated from a mantle plume similar to the source of OIB, with partial melts of this mantle mixing significantly with the subcontinental lithospheric mantle (Xu et al., 2007). Emeishan basalts thus can be used to define a mixing trend between the OIB-like asthenospheric mantle and the continental lithospheric mantle sources using La/Nb and $\varepsilon Nd_{(T)}$ covariations (Fig. 5). This mixing trend is nearly identical to that constructed for basalts of the southwest Basin and Range in the western United States by mixing of two components, the OIB-like asthenospheric and lithospheric mantle, which is inferred from the good correlation not only between $\varepsilon Nd_{(T)}$ and La/Nb, but also $\varepsilon Nd_{(T)}$ and $^{87}Sr/^{86}Sr$ (DePaolo and Daley, 2000). Ningyuan basalts and the great majority of Cathaysia Folded Belt basalts (except those from Huichang) fall along this trend, suggesting that they are derived in a similar way. North Guangdong mafic dikes are mostly clustered near the OIB-like asthenosphere end;

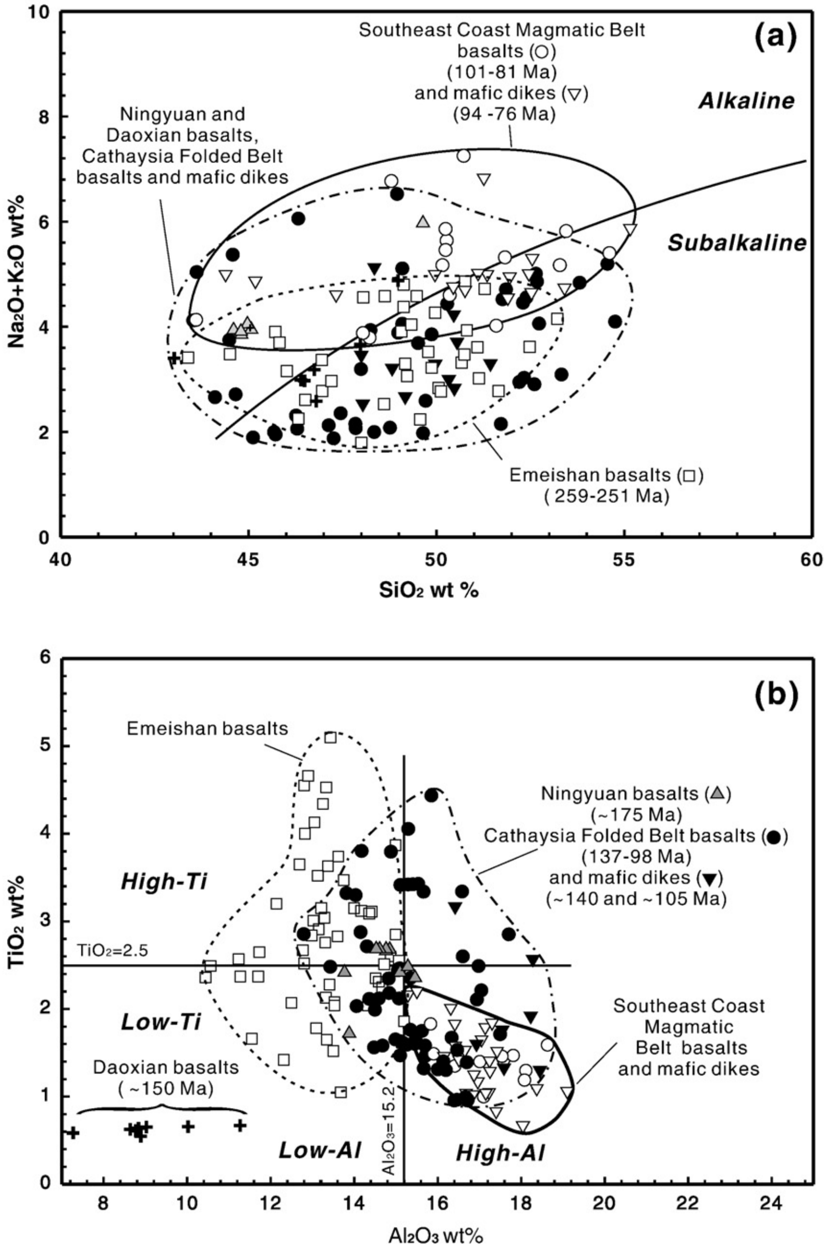

Fig. 3. Major element distribution for Mesozoic basaltic rocks in South China based on (a) Na_2O+K_2O vs. SiO_2 plots and (b) TiO_2 vs. Al_2O_3 plots. The division line of alkaline and subalkaline rocks is taken from Wilson (1989). Some published data of Emeishan basalts (Xu et al., 2001), Jurassic and Cretaceous Cathaysia Interior and Cathaysia Folded Belt basalts (Li et al., 2003, 2004; Xiong et al., 2003; Wang et al., 2005) and mafic dikes (Li and McCulloch, 1998) are also included.

a few having higher La/Nb ratios are explained by crustal contamination through dike injections (Li and McCulloch, 1998). On this basis, an OIB-like asthenospheric mantle component deduced from Emeishan and Ningyuan basalts and north Guangdong mafic dikes has a low value of La/Nb (0.6), and high $\varepsilon Nd_{(T)}$ (+5) in association with low initial $^{87}Sr/^{86}Sr$ (0.704). Interestingly, the Late Cenozoic basalts in Zhejiang–Fujian region, which are spatially associated with these Mesozoic rocks have also been interpreted as OIB-like basalts and exhibit similar values (La/Nb = 1.0, $\varepsilon Nd_{(T)}$ = +5, and initial $^{87}Sr/^{86}Sr$ = 0.704) for relatively uncontaminated samples (Ho et al., 2004). Trace element and isotopic characteristics of the subcontinental lithospheric mantle component, although not well defined because of the paucity of data at the low $\varepsilon Nd_{(T)}$ end, may label a few of the basalts in the Southeast Coast Magmatic Belt (La/Nb = 1.7 and $\varepsilon Nd_{(T)}$ = −9.5) (Fig. 5). However, there could be slight differences in the Cathaysia Folded Belt as the limit of the range of composition of these basalts (La/Nb = 1.6 and $\varepsilon Nd_{(T)}$ = −6) lies somewhat away from the lithosphere end-member.

On the other hand, the great majority of Southeast Coast Magmatic Belt basalts and mafic dikes have elevated La/Nb ratios which deviate significantly from this asthenosphere–lithosphere mantle mixing trend and are widespread over a field similar to the West Great Basin basalts (Fig. 5). The overall heterogeneity is explained either by crustal contamination (e.g., a few north Guangdong mafic dikes as mentioned), or by involvement of a subduction component. Just as the West Great Basin basalts were explained by a mixing between asthenosphere-derived magmas (Basin and Range basalts) and lithospheric mantle-derived magmas enriched via fluids expelled from a subducted slab (Fitton et al., 1991; Rogers et al., 1995) or subducted pelagic-to-turbidite sediments (Beard and Johnson, 1997), Southeast Coast Magmatic Belt basalts and a few of the stage-2 Cathaysia Folded

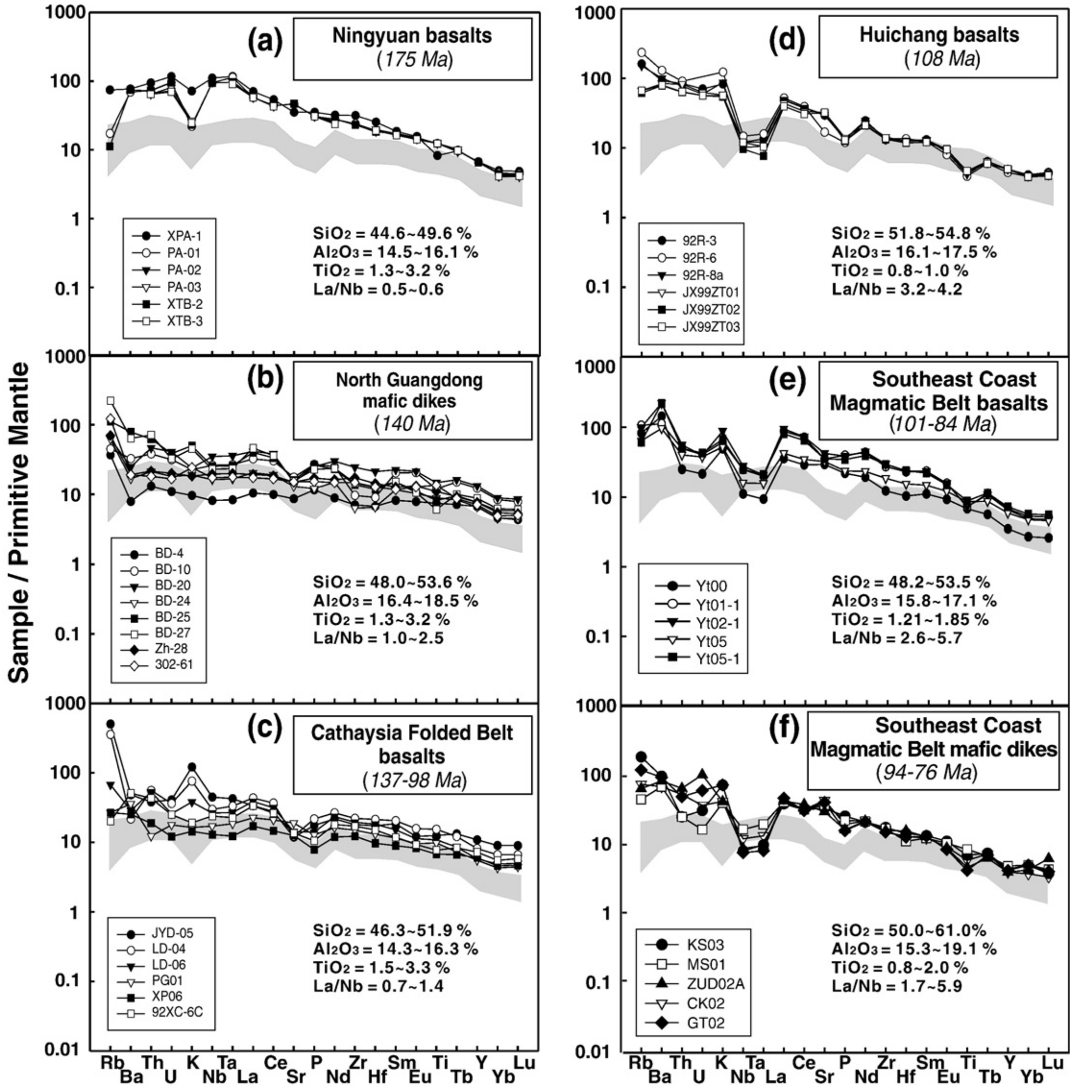

Fig. 4. Primitive mantle-normalized multi-element distribution pattern for Mesozoic basaltic rocks in South China, including (a) Ningyuan basalts (Li et al., 2004); (b) north Guangdong mafic dikes (Li and McCulloch, 1998); (c) Cathaysia Folded Belt basalts (except Huichang); (d) Huichang basalts; (e) Southeast Coast Magmatic Belt basalts and (f) mafic dikes. The shaded pattern represents the Emeishan basalts (Xu et al., 2001; Ali et al., 2005). Primitive mantle normalizing values are from McDonough and Sun (1995).

Belt basalts (Huichang) can likewise be regarded as derivatives of subduction-modified basic magmas. As for Daoxian basalts, they are better explained by crustal contamination based on the Pb isotopic compositions in the following section.

Involvement of subducted sediment in the mantle of South China is further examined by using Pb isotope ratios, which are especially sensitive indicators. Here we use the deep-sea sediments of the Philippine Sea Plate (Yu, 2005) as the reference. The oldest oceanic crust of the Philippine Sea Plate and northwest Pacific Plate were reported to be Late Jurassic to Early Cretaceous (Deschamps et al., 2000; Hirano et al., 2006). These deep-sea sediments are chosen to represent material derived from the adjacent Asiatic continent at the time when the west Pacific subduction system was operating during the Late Mesozoic. When Pb isotope ratios are plotted with Nd isotope ratios, several features are noted: (1) There are no discernible differences between the Emeishan and Cathaysia Folded Belt basalts; (2) Daoxian basalts have elevated $^{207}Pb/^{204}Pb$ ratios like the case of some Deccan Traps basalts, indicating a moderate but significant influence from the upper crust (Mellusoa et al., 2006); (3) Ningyuan basalts are characterized by distinctive Nd and Pb isotope compositions close to Basin and Range basalts; (4) Huichang basalts have the lowest values, close to deep-sea sediments for all Pb isotopic ratios among the Cathaysia Interior and Cathaysia Folded Belt samples, and (5) Southeast Coast Magmatic Belt basalts, comparable to the West Great Basin basalts, are restricted to a small field sitting between Cathaysia Folded Belt basalts and deep-sea sediments (Fig. 6).

Some interpretations can be readily made. Due to overlapping of these isotopic compositions, Cathaysia Folded Belt basalts are derived from compositionally similar mantle components to Emeishan basalts (except Daoxian basalts that may involve a significant upper crust component); Ningyuan samples are comparable with Basin and Range basalts and are the least contaminated basalts derived from the asthenosphere that has Pb isotopic compositions that deviate slightly from Emeishan and Cathaysia Folded Belt basalts; and Southeast Coast Magmatic Belt (+Huichang) basalts could be mixing products between Cathaysia Folded Belt mantle melts and deep-sea sediments — indicative of magma generation from subduction-modified sources. Therefore, the Mesozoic mantle of the entire east–west basalt array in South China seems to be related to the eastward migration of the Emeishan mantle, with possible asthenospheric upwelling during the Early Jurassic when the rift system developed (Zhou et al., 2006). Also the Cretaceous Southeast Coast Magmatic Belt mantle reflects a

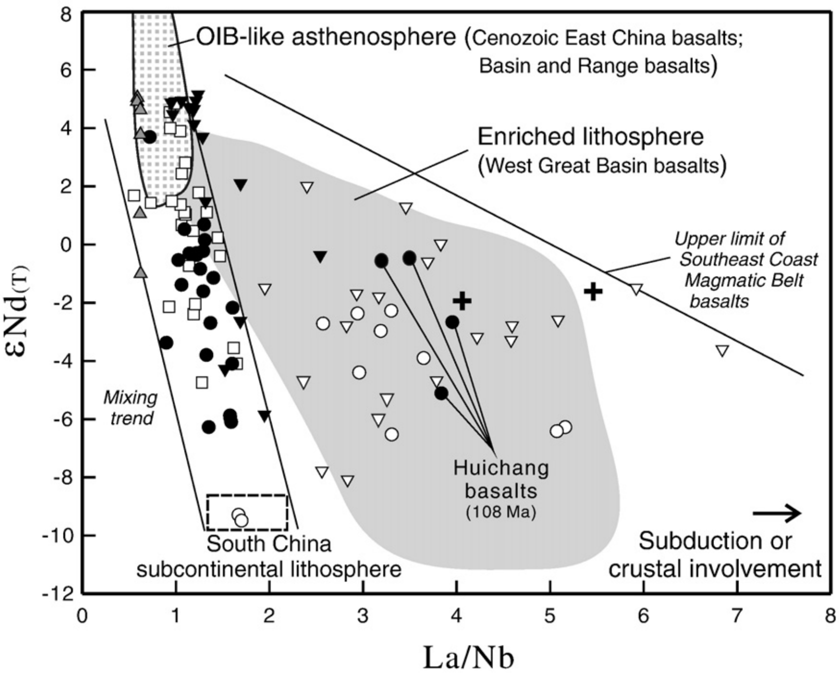

Fig. 5. $\varepsilon Nd_{(T)}$ vs. La/Nb plots for Mesozoic basaltic rocks in South China revealing that Cathaysia Folded Belt basalts (except Daoxian and Huichang samples) fall in the narrow asthenosphere–lithosphere mantle mixing trend constructed from Emeishan and Ningyuan basalts, whereas Southeast Coast Magmatic Belt basalts have a much wider distribution. Asthenosphere- and enriched lithosphere (subduction-induced)-derived basalts of western United States (Fitton et al., 1991; Rogers et al., 1995), in dotted and shaded areas, respectively, are shown for comparison. The Late Cenozoic Zhejiang–Fujian basalts (Ho et al., 2004) fall into the ocean island basalt (OIB)-like asthenosphere field. Unmodified South China subcontinental lithosphere is inferred from the combination of low $\varepsilon Nd_{(T)}$ and high La/Nb (DePaolo and Daley, 2000). Symbols are same as in Fig. 3.

simple subduction system as compared to the West Great Basin, which probably requires an additional, less radiogenic (lower $^{206}Pb/^{204}Pb$) composition than the pelagic sediments (Fig. 6c).

The distance between the Cathaysia Folded Belt basaltic areas and the presumed subduction zone is relatively short (Fig. 1a) and the time lag between the Cathaysia Folded Belt and Southeast Coast Magmatic Belt basaltic activity is rather small (<10 Myr). However, few of the Cathaysia Folded Belt basalts (e.g., Huichang basalts) have geochemical and isotopic characters similar to the Southeast Coast Magmatic Belt basalts, showing that little of the Cathaysia Folded Belt mantle had undergone mantle wedge-subducted plate interactions like those in the Southeast Coast Magmatic Belt. This suggests that a large part of the Late Mesozoic Cathaysia Folded Belt mantle have been undisturbed by the subduction system before 108 Ma. This is in accord with the occurrence of two Early Cretaceous gabbroic intrusions in south Fujian, with K–Ar ages of 130–126 Ma and 108 Ma, respectively, which were also derived from a mantle source unmodified by subduction components (Zhao et al., 2007).

6. Implications for Mesozoic tectonic evolution in South China

Age, geochemical and isotopic characteristics of all the Mesozoic basaltic rocks in South China are summarized in Table 1, from which the inferred magma sources for these basalts are proposed. Here we emphasize two major points for Cathaysia Interior and Cathaysia Folded Belt basalts: (1) they decrease in age eastward in the Mesozoic, and (2) except the Huichang basalts, they were mainly mixtures of melts derived from OIB-like asthenospheric mantle and the South China subcontinental lithosphere mantle without being significantly modified by the crust during their transit to the surface. Any tectonic model applied to Mesozoic Cathaysia must satisfy these criteria.

It is generally accepted that there was magmatic quiescence during the period 205 to 180 Ma, and new magmatism began with intraplate basaltic eruptions in the Cathaysia Interior, accompanied by intrusions of syenitic and A-type granites (180–170 Ma) in the Cathaysia Folded Belt (Li et al., 2003, 2004; Zhou et al., 2006). The model of Li and Li (2007) relates all the Triassic to Cretaceous granitoids in the Cathaysia Block to paleo-Pacific subduction and ascribed the generation of Late Jurassic granitoids to "slab foundering" as a consequence of rollback of the retreating flat subduction. Based on the proposed flat-to-normal slab variations in the Central Andes, western North America and southeastern Tibet, the final thermal activity right before the magmatic gap is characterized by the generation of adakites under thickened arc crust conditions. The resuming magmatism consists of "normal" calc-alkaline rocks (Kay and Mpodozis, 2002; Saleeby, 2003; Wen et al., 2008). However, there are no known Late Triassic adakitic rocks in the Cathaysia Block, and the resumption of syenitic and A-type granitic intrusions cannot support the conclusion that the granitic magmatic evolution during the Mesozoic followed such a pattern. The flat subduction model for the paleo-Pacific plate is therefore not convincing.

On the other hand, Zhou et al. (2006) considered that Triassic granites were influenced by a paleo-Tethyan subduction system, and that the occurrence of the Early Jurassic basaltic, syenitic and A-type granitic rocks marked the beginning of the paleo-Pacific tectonic regime, and formation of voluminous Late Jurassic granitoids was controlled by rift-type intraplate magmatism, but no tectonic evolution model was proposed. Our geochemical and isotopic data demonstrate that mantle beneath the Cathaysia Interior and Cathaysia Folded Belt is characterized by a rather homogeneous domain, distinctly different from the Southeast Coast Magmatic Belt that has been modified by the paleo-Pacific subduction system. Age data indicate that such mantle remained undisturbed during the Jurassic (Table 1). Therefore, the east-west basalt array represents an eastward trace of continental extension through time, most likely subjected to the progressive Triassic continent–continent collision between the Indochina and South China Blocks, or the so-called Indosinian orogeny (e.g., Carter et al., 2001). Appearance of OIB-like basalts in some places along the east–west basalt array (e.g., south Hunan and north Guangdong) is an indication of extension that gives way to asthenospheric sources. By asthenosphere upwelling associated with constant underplating of mafic magmas under the extension regime, the

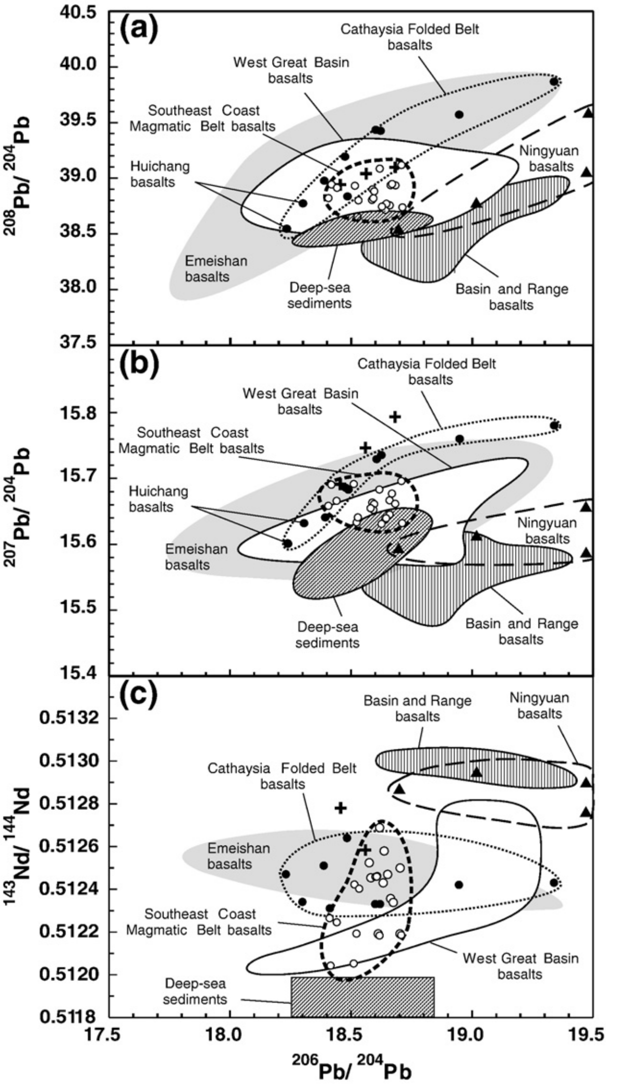

Fig. 6. Variations of Pb and Nd isotopic compositions for Mesozoic basaltic rocks in South China. Data sources are shown in Appendix 2 except for the deep-sea sediments of the Philippine Sea plate that are taken from Yu (2005), and the Basin and Range and West Great Basin basalts from Kempton et al. (1991). Symbols are the same as in Fig. 3.

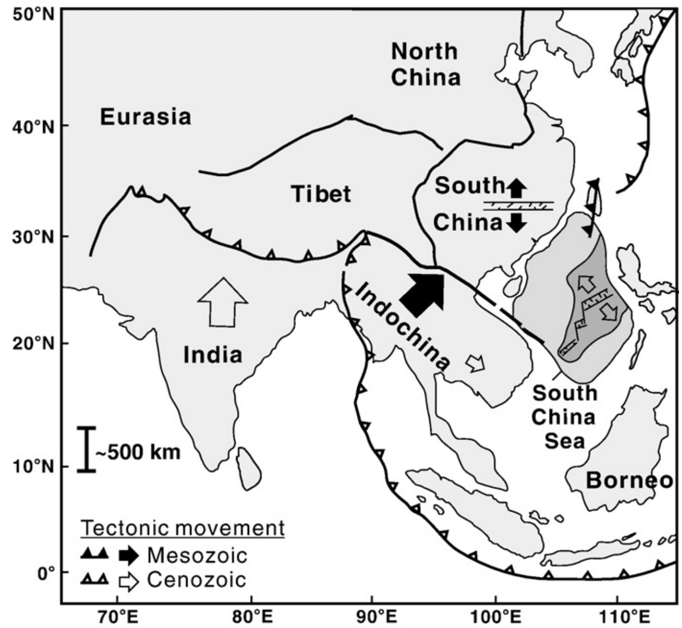

Fig. 7. Schematic diagram showing the tectonic configuration of the Oligocene–Early Miocene seafloor spreading in the South China Sea relative to the Early Cenozoic India–Eurasia continent collision (Lee and Lawver, 1995) and the Jurassic extension in the Cathaysia Block (South China) relative to the Triassic Indochina–South China continent collision (Indosinian orogeny). On the basis of the collision–extension relationship, the latter may be an earlier analogue of the former although the scale is smaller. Hence, Jurassic tectonism in South China is explained as mainly due to post-Indosinian continental extension. Open symbols denote Cenozoic and solid symbols denote Triassic/Jurassic direction of plate movements.

overlying crustal materials were eventually melted to form vast Jurassic east–west striking granitic batholiths in the Cathaysia Folded Belt in a relatively short period of time at 160±5 Ma as the geotherm crossed the solidus of preexisting (mainly Caledonian) granitic crustal material. As for the Early Jurassic syenitic and A-type granitic rocks, they are simply the fractionated derivatives of alkaline gabbro — the intrusive equivalent of alkaline basalt (Hsieh et al., 2008).

The Jurassic extensional environment in the Cathaysia Block after the Triassic Indochina-South China continent collision may be an earlier analogue of Oligocene–Early Miocene seafloor spreading in the South China Sea after the Early Cenozoic India–Eurasia continent collision (Fig. 7). The indentation experiment of Tapponnier et al. (1982) has been used to describe the tectonic evolution in Southeast Asia, mainly including southeastward extrusion of the Indochina Block and opening of the South China Sea (marked by open arrows in Fig. 7) subsequent to the beginning of the India–Eurasia continent collision (Lee and Lawver, 1995). On the basis of the relative position and

Table 1
Summary of age, geochemical and isotopic characteristics of Mesozoic basaltic rocks in S China

Tectonic unit	Emeishan[1]	Cathaysia Interior[2]		Cathaysia Folded Belt		SCMB
		Ningyuan	Daoxian	Stage 1	Stage 2	
Age (Ma)	259–251	~175	~150	137–123	108–98	101~76
Lithology	Subalk (+alk) flood basalt	Alkaline basalt	High-Mg basalt**	Subalk (+alk) basalt	Subalk+alk+high-Al basalt	High-Al basalt
TiO_2*	H+L	H	L	H+(L)	L+(H)	L
Al_2O_3*	L	L	L	L+(H)	H+(L)	H
La/Nb	0.5~1.6	0.5~0.6	4~5.5	0.8~1.6	0.7~4	2~7
$(^{87}Sr/^{86}Sr)_i$	0.704~0.706	ca. 0.704	ca. 0.706	0.706–0.710	0.705~0.708	0.707~0.711
$\varepsilon Nd_{(T)}$	−5~+5	ca. +5	ca. −2	−6.3~+0.1	−5.1~+3.7	−9.5~−2.7
$^{206}Pb/^{204}Pb$	17.8~19.3	19.5	18.5~18.7	18.5~19.3	18.2~18.5	18.4~18.7
$^{207}Pb/^{204}Pb$	15.6~15.7	15.6~15.7	15.7~15.8	15.7~15.8	15.6~15.7	15.6~15.7
$^{208}Pb/^{204}Pb$	38.0~39.9	39.4~39.6	38.8~39.1	39.0~39.9	38.6~38.8	38.6~39.0
Interpreted magma source	Plume+lithosphere mantle	OIB-like asthenosphere±lithosphere mantles±crust contamination		OIB-like asthenosphere+lithosphere± subduction-modified mantles		Subduction-modified mantle

*Divisions for H (high) and L (low) are 2.5 wt.% for TiO_2 and 15.2 wt.% for Al_2O_3; those in the parenthesis are present in lesser amount. ** MgO>16 wt.%. 1–2: Data sources are included in Appendix 2.
$(^{87}Sr/^{86}Sr)_i$: initial $^{87}Sr/^{86}Sr$. SCMB: Southeast Coast Magmatic Belt.

orientation of the collision zone and spreading axis, as well as the time sequence of these tectonic events, the configuration of the Jurassic extensional (rifting) system in the Cathaysia Block can be regarded as analogue of the South China Sea spreading, with the only difference being that continental extension was not vigorous enough to trigger seafloor spreading. In conclusion, we modify the proposition of Zhou et al. (2006) by interpreting the Jurassic granitoids in South China as products of post-orogenic (Indosinian) magmatism, while the orogenic magmatism is marked by the Triassic strongly peraluminous (partly haplo-) granites in Hunan and Guangxi (Li and Li, 2007).

7. Conclusions

The orogenic cycles related to the sequence of tectonic events in association with paleo-Pacific subduction are best reflected by time-dependent granitic intrusions and basalt/rhyolite bimodal eruptions in the coastal area (Chen et al., 2004, 2008). The syn-orogenic stage is reflected by the tonalite–trondhjemite–granodiorite assemblage that was emplaced at 24 – 28 km depth west of the Southeast Coast Magmatic Belt between 140–110 Ma, i.e. the thickened crust stage. The post-orogenic stage is characterized by shallow intrusions (6–8 km depth) of 110–99 Ma granitoids and succeeding 100–90 Ma A-type granites. We now consider volcanic eruptions of Southeast Coast Magmatic Belt basalts to have been generated in the closing (anorogenic) stage of the magmatic cycle. In other words, the so-called Late Yanshanian orogeny, like some other contemporaneous magmatic and orogenic belts of the circum-Pacific continental margin (e.g., Rubin et al., 1995), underwent independent and complete cycles of magmatism within a time span of ~50 Myr.

Acknowledgements

Drs. Ching-Hua Lo and Huai-Jen Yang are thanked for their arrangements for $^{40}Ar/^{39}Ar$ age dating and Sr and Nd isotope ratio measurements, respectively. Prof. John Suppe (formerly at Princeton and now Taipei) and Dr. George Burr (Tucson) are thanked for their comments and corrections of the early manuscript. Drs. Pat Castillo (UCSD), Mei-Fu Zhou (Hong Kong) and Andrew Kerr (Editor-in-chief) are thanked for their thoughtful reviews and constructive comments. This work is supported by research grants from the National Science Council, Taiwan (NSC89, 90, 91-2116-M-002-047, 012 and 032/Chen) and the Japanese Grant-in-Aid for Scientific Research (C: No.13640483/Shinjo).

Appendixes A and B. Supplementary data

Supplementary data associated with this article can be found, in the online version, at doi:10.1016/j.lithos.2008.06.009.

References

Ali, J.R., Thompson, G.M., Zhou, M.-F., Song, X., 2005. Emeishan large igneous province, SW China. Lithos 79, 475–489.
Beard, B.L., Johnson, C.M., 1997. Hafnium isotope evidence for the origin of Cenozoic basaltic lavas from the southwestern United States. Journal of Geophysical Research 102, 20149–20178.
Berndt, J., Koepke, J., Holtz, F., 2005. An experimental investigation of the influence of water and oxygen fugacity on differentiation of MORB at 200 MPa. Journal of Petrology 46, 135–167.
Carter, A., Roques, D., Bristow, C., Kinney, P., 2001. Understanding Mesozoic accretion in Southeast Asia: significance of Triassic thermotectonism (Indosinian orogeny) in Vietnam. Geology 29, 211–214.
Chen, C.-H., Lin, W., Lan, C.Y., Lee, C.Y., 2004. Geochemical and Sr, Nd isotopic characteristics and tectonic implications for three stages of igneous rock in the Late Yanshanian (Cretaceous) orogeny, SE China. Transaction of the Royal Society of Edinburgh-Earth Sciences 95, 237–248.
Chen, C.-H., Lu, H.Y., Lin, W., Lee, C.Y., 2006. Thermal event records in SE China coastal areas: Constraints from monazite ages of beach sands from two sides of the Taiwan Strait. Chemical Geology 231, 118–134.
Chen, C.-H., Lee, C.Y., Lu, H.Y., Hsieh, P.S., 2008. Generation of Late Cretaceous silicic rocks in SE China coastal areas: age, major element and numerical simulation constraints. Journal of Asian Earth Sciences 31, 479–498.
Crawford, A.J., Falloon, T.J., Eggins, S., 1987. The origin of island arc high-alumina basalts. Contributions to Mineralogy and Petrology 97, 417–430.
DePaolo, D.J., Daley, E.E., 2000. Neodymium isotopes in basalts of the southwest basin and range and lithospheric thinning during continental extension. Chemical Geology 169, 157–185.
Deschamps, A., Monie, P., Lallemand, S., Hsu, S.-K., Yeh, K.Y., 2000. Evidence for Early Cretaceous oceanic crust trapped in the Philippine Sea Plate. Earth and Planetary Science Letters 179, 503–516.
Fitton, J.G., James, D., Leeman, W.P., 1991. Basic magmatism associated with Late Cenozoic extension in the western United States: compositional variations in space and time. Journal of Geophysical Research 96, 13,693–13,711.
Hirano, N., Takahashi, E., Yamamoto, J., Abe, N., Ingle, S.P., Kaneoka, I., Hirata, T., Kimura, J., Ishii, T., Ogawa, Y., Machida, S., Suyehiro, K., 2006. Volcanism in response to plate flexure. Science 313, 1426–1428.
Ho, K.S., Chen, J.C., Lo, C.H., Zhao, H.L., 2004. ^{40}Ar–^{39}Ar dating and geochemical characteristics of late Cenozoic basaltic rocks from the Zhejiang–Fujian region, SE China: eruption ages, magma evolution and petrogenesis. Chemical Geology 197, 287–318.
Hsieh, P.S., Chen, C.-H., Yang, H.J., Lee, C.Y., 2008. Petrogenesis of the Nanling Mountains granites from South China: constraints from systematic apatite geochemistry and whole-rock geochemical and Sr–Nd isotope compositions. Journal of Asian Earth Sciences. doi:10.1016/j/jeaes.2008.02.002.
Kay, S.M., Mpodozis, C., 2002. Magmatism as a probe to the Neogene shallowing of the Nazca plate beneath the Chilean flat-slab. Journal of South America Earth Sciences 15, 39–57.
Kempton, P.D., Fitton, J.G., Hawkesworth, C.J., Ormerod, D.S., 1991. Isotopic and trace element constraints on the composition and evolution of the lithosphere beneath the southwestern United States. Journal of Geophysical Research 96, 13713–13735.
Lee, T.Y., Lawver, L.A., 1995. Cenozoic plate reconstruction of Southeast Asia. Tectonophysics 251, 85–138.
Li, Z.X., Li, X.H., 2007. Formation of the 1300 km-wide intracontinental orogen and postorogenic magmatic province in Mesozoic South China: a flat-slab subduction model. Geology 35, 179–182.
Li, X.H., McCulloch, M.T., 1998. Geochemical characteristics of Cretaceous mafic dikes from northern Guangdong, SE China: age, origin and tectonic significance. In: Flower, M.F.J., et al. (Ed.), Mantle Dynamics and Plate Interactions in East Asia. AGU Geodynamics Series, vol. 27, pp. 405–419.
Li, X.H., Chen, Z., Liu, D., Li, W.X., 2003. Jurassic gabbro-granite-syenite suites from southern Jiangxi Province, SE China: age, origin, and tectonic significance. International Geology Review 45, 898–921.
Li, X.H., Chung, S.L., Zhou, H., Lo, C.H., Liu, Y., Chen, C.H., 2004. Jurassic intraplate magmatism in southern Hunan-eastern Guangxi: dating, geochemistry, Sr–Nd isotopes and implications for the tectonic evolution of SE China. In: Malpas, J., et al. (Ed.), Aspects of the Tectonic Evolution of China, vol. 226. Geological Society, London, pp. 193–216. Special Publications.
Lo, C.H., Lee, C.Y., 1994. $^{40}Ar/^{39}Ar$ method of K–Ar age determination of geological samples using Tsing-Hua Open-pool Reactor (THOR). Journal of the Geological Society of China 37, 143–164.
Martin, H., Bonin, B., Capdevila, R., Jahn, B.M., Lameyre, J., Wang, Y., 1994. The Kuiqi peralkaline granitic complex (SE China): petrology and geochemistry. Journal of Petrology 35, 983–1015.
McDonough, W.F., Sun, S.S., 1995. The composition of the earth. Chemical Geology 120, 223–253.
Mellusoa, L., Mahoney, J.J., Dallai, L., 2006. Mantle sources and crustal input as recorded in high-Mg Deccan Traps basalts of Gujarat (India). Lithos 89, 259–274.
Ratschbacher, L., Hacker, B.R., Webb, L.E., McWilliams, M., Ireland, T., Dong, S., Calvert, A., Chateigner, D., 2000. Exhumation of the ultrahigh-pressure continental crust in east central China: Cretaceous and Cenozoic unroofing and the Tan-Lu fault. Journal of Geophysical Research 105, 13303–13338.
Rogers, N.W., Hawkesworth, C.J., Ormerod, D.S., 1995. Late Cenozoic basaltic magmatism in the Western Great Basin, California and Nevada. Journal of Geophysical Research 100, 10287–10302.
Rubin, C.M., Miller, E.L., Toro, J., 1995. Deformation of the northern circum-Pacific margin: variations in tectonic style and plate-tectonic implications. Geology 23, 897–900.
Saleeby, J., 2003. Segmentation of the Laramide slab — evidence from the southern Sierra Nevada region. Geological Society of America Bulletin 115, 655–668.
Tapponnier, P., Peltzer, G., Le Dain, A.Y., Armijo, R., 1982. Propagating extrusion tectonics in Asia: new insights from simple experiments with plasticine. Geology 10, 611–616.
Turner, S., Hawkesworth, C., 1997. Constraints on flux rates and mantle dynamics beneath island arcs from Tonga-Kermadec lava geochemistry. Nature 389, 568–573.
Wang, Y., Fan, W., Guo, F., Peng, T., Li, C., 2003. Geochemistry of Mesozoic mafic rocks adjacent to the Chenzhou-Linwu fault, South China: implications for the lithospheric boundary between the Yangtze and Cathaysia blocks. International Geology Review 45, 263–286.
Wang, Y., Fan, W., Peng, T., Guo, F., 2005. Elemental and Sr–Nd isotopic systematics of the early Mesozoic volcanic sequence in southern Jiangxi Province, South China: petrogenesis and tectonic implications. International Journal of Earth Sciences 94, 53–65.
Wen, D.-R., Chung, S.L., Song, B., Iizuka, Y., Yang, H.-J., Ji, J., Liu, D., Gallet, S., 2008. Late Cretaceous Gangdese intrusions of adakitic geochemical characteristic, SE Tibet: petrogenesis and tectonic implications. Lithos. doi:10.1016/j.lithos.2008.02.005.
Wilson, M., 1989. Igneous Petrogenesis. Unwin Hyman, London. 466pp.
Woodhead, J.D., Volker, F., McCulloch, M.T., 1995. Routine lead isotope determinations using a lead-207–lead-204 double spike: a long-term assessment of analytical precision and accuracy. Analyst 120, 35–39.

Xie, X., Xu, X., Zou, H., Jiang, S., Zhang, M., Qiu, J., 2006. Early J2 basalts in SE China: incipience of large-scale Late Mesozoic magmatism. Science in China Series D (Earth Sciences) 49, 796–815.

Xiong, X.L., Li, X.H., Xu, J.F., Li, W.X., Zhao, Z.H., Wang, Q., Chen, X.M., 2003. Extremely high-Na adakite-like magmas derived from alkali-rich basaltic underplate: the Late Cretaceous Zhantang andesites in the Huichang Basin, SE China. Geochemical Journal 37, 233–252.

Xu, Y., Chung, S.L., Jahn, B.-M., Wu, G., 2001. Petrologic and geochemical constraints on the petrogenesis of Permo-Triassic Emeishan flood basalts in southwestern China. Lithos 58, 145–168.

Xu, X., O'Reilly, S.Y., Griffin, W.L., Deng, P., Pearson, H.J., 2005. Relict Proterozoic basement in the Nanling Mountains (SE China) and its tectonothermal overprinting. Tectonics 24, TC2003. doi:10.1029/2004TC001652.

Xu, J.-F., Suzuki, K., Xu, Y.-G., Mei, H.-J., Li, J., 2007. Os, Pb, and Nd isotope geochemistry of the Permian Emeishan continental flood basalts: insights into the source of a large igneous province. Geochimica et Cosmochimica Acta 71, 2104–2119.

Yu, C., 2005. Lead isotope compositions of subducting sediments around the Pacific. Master thesis, Dept Geol., Washington State Univ., 112pp.

Zhao, J.H., Hu, R., Zhou, M.F., Liu, S., 2007. Elemental and Sr–Nd–Pb isotopic geochemistry of Mesozoic mafic intrusions in southern Fujian Province, SE China: implications for lithospheric mantle evolution. Geological Magazine 144, 937–952.

Zhou, X.M., Li, X.W., 2000. Origin of Late Mesozoic rocks in southeastern China: implications for lithosphere subduction and underplating of mafic magmas. Tectonophysics 326, 269–287.

Zhou, X., Sun, T., Shen, W., Shu, L., Niu, Y., 2006. Petrogenesis of Mesozoic granitoids and volcanic rocks in South China: a response to tectonic evolution. Episodes 29, 26–33.